JOURNAL OF GEOPHYSICAL RESEARCH, VOL. 111, A11214, doi:10.1029/2006JA011657, 2006

Outward radial diffusion driven by losses at magnetopause

Y. Y. Shprits,[1] R. M. Thorne,[1] R. Friedel,[2] G. D. Reeves,[2] J. Fennell,[3] D. N. Baker,[4] and S. G. Kanekal[4]

Received 8 February 2006; revised 22 May 2006; accepted 14 June 2006; published 14 November 2006.

[1] Loss mechanisms responsible for the sudden depletions of the outer electron radiation belt are examined based on observations and radial diffusion modeling, with L^*-derived boundary conditions. SAMPEX data for October–December 2003 indicate that depletions often occur when the magnetopause is compressed and geomagnetic activity is high, consistent with outward radial diffusion for $L^* > 4$ driven by loss to the magnetopause. Multichannel Highly Elliptical Orbit (HEO) satellite observations show that depletions at higher L occur at energies as low as a few hundred keV, which excludes the possibility of the electromagnetic ion cyclotron (EMIC) wave-driven pitch angle scattering and loss to the atmosphere at $L^* > 4$. We further examine the viability of the outward radial diffusion loss by comparing CRRES observations with radial diffusion model simulations. Model-data comparison shows that nonadiabatic flux dropouts near geosynchronous orbit can be effectively propagated by the outward radial diffusion to $L^* = 4$ and can account for the main phase depletions of outer radiation belt electron fluxes.

Citation: Shprits, Y. Y., R. M. Thorne, R. Friedel, G. D. Reeves, J. Fennell, D. N. Baker, and S. G. Kanekal (2006), Outward radial diffusion driven by losses at magnetopause, *J. Geophys. Res.*, *111*, A11214, doi:10.1029/2006JA011657.

1. Introduction

[2] Flux variations in the radiation belts can generally be divided into two categories: adiabatic or reversible changes and nonadiabatic or irreversible. Adiabatic changes in electron fluxes occur when the magnetic field changes slowly compared to the timescale associated with the particle adiabatic invariants [*Roederer*, 1970]. When the magnetic field decreases slowly due to an increase in the storm-time ring current, electrons move out to conserve the third invariant, and lose energy to conserve the first adiabatic invariant. When either the gradient of the energy spectrum or the radial gradient is steep, the radial displacement of electrons will result in significant changes of electron fluxes at a fixed radial distance and energy, as observed by spacecraft [*Li et al.*, 1997; *Kim and Chan*, 1997; *Reeves et al.*, 1998].

[3] To explain the net effect of adiabatic variations, it is instructive to consider two extreme cases in which particles move outward due to decreases in magnetic field. If there is no radial gradient in phase space density (PSD), but there is a declining energy spectrum, the spacecraft will see fewer particles at a fixed energy because they originate from an initial (smaller) population at higher energies. On the other hand, if the energy spectrum is flat but there is an inward radial gradient (more PSD at lower L values), the spacecraft will measure an increase in electron fluxes. The magnitude of the adiabatic flux variations will depend on the steepness of the energy spectrum, radial gradients, the magnitude of the disturbance in the field, and the background magnetic field. The strongest effect is usually at higher L shells where the background magnetic field tends to be weaker [*Kim and Chan*, 1997]. For many storms, fluxes do not return to the original prestorm values, which indicates that nonadiabatic losses occur during storms [*McAdams and Reeves*, 2001; *Onsager et al.*, 2002; *Reeves et al.*, 2003; *Green et al.*, 2004]. The net effect of losses during storms could be compensated by the various enhanced sources of electrons [*Reeves et al.*, 2003].

[4] Significant progress has been made in resent years in quantifying nonadiabatic loss mechanisms in the radiation belts. Losses inside the plasmasphere are predominantly due to scattering by plasmaspheric hiss with loss timescales on the order of 5 to 10 days [*Lyons et al.*, 1972; *Albert*, 1994; *Abel and Thorne*, 1998]. *Meredith et al.* [2004] also demonstrated that the intensity of the hiss and consequently the rate of pitch angle scattering are correlated with the level of geomagnetic activity.

[5] From radial diffusion simulations, *Shprits et al.* [2005] concluded that effective losses in the heart of the radiation belts (where the outer radiation belt fluxes maximize) usually occur on the timescale of a day, which is much shorter than timescales associated with plasmaspheric hiss. Theoretical estimates of the scattering rates indicate that losses due to chorus waves occur throughout the outer radiation belt [*Albert*, 2005; *Horne et al.*, 2005a; *Thorne et al.*, 2005b]. Combined SAMPEX and Polar observations also show that microburst precipitation, which is thought to be produced by bursty chorus waves [*Lorentzen et al.*,

[1]Department of Atmospheric and Oceanic Sciences, University of California, Los Angeles, California, USA.
[2]Los Alamos National Laboratory, Los Alamos, New Mexico, USA.
[3]The Aerospace Corporation, El Segundo, California, USA.
[4]Laboratory for Atmospheric and Space Physics, University of Colorado, Boulder, Colorado, USA.

0148-0227/06/2006JA011657$09.00

2001], can provide electron losses on the scale of a day [*O'Brien et al.*, 2004; *Thorne et al.*, 2005b].

[6] EMIC waves could possibly provide fast localized losses on the timescale of hours [*Thorne and Kennel*, 1971; *Albert*, 2003; *Summers and Thorne*, 2003]. These waves are preferentially excited in the high-density plasmasphere, along the duskside plasmapause [*Horne and Thorne*, 1993; *Kozyra et al.*, 1997; *Horne and Thorne*, 1997; *Jordanova et al.*, 2001a, 2001b; *Erlandson and Ukhorskiy*, 2001], during enhanced convective injection of ring current ions. In the vicinity of the plasmapause, the minimum electron energy for resonance can drop to 500 keV [*Meredith et al.*, 2003; *Summers and Thorne*, 2003; *Albert*, 2003]. Resonant relativistic electrons only briefly traverse the dusk side region of intense EMIC waves, but may produce very rapid precipitation events which are strongly localized in MLT. Precipitation due to EMIC waves may be also related to the bursts of hard X rays seen by balloon-borne instruments [*Lorentzen et al.*, 2000; *Millan et al.*, 2002].

[7] Even though radial diffusion rates are strongest during the main phase of the storm and are capable of effectively transporting electrons to lower L shells and accelerating them, electron fluxes are commonly observed to decrease during the main phase of a storm [e.g., *Nagai*, 1988; *Mathie and Mann*, 2000; *O'Brien et al.*, 2001; *Onsager et al.*, 2002]. *Desorgher et al.* [2000] performed guiding center and radial diffusion simulations of the 26 March 1995 storm. Their model results significantly underestimated the observed fluxes at $L > 5$. The discrepancies between the results and observations were attributed to a simplified treatment of the magnetopause as a perfect absorber and neglect of the pitch angle diffusion. *Brautigam and Albert* [2000] and *Miyoshi et al.* [2003] performed radial diffusion simulations of individual storms with variable outer boundary conditions derived from geosynchronous satellite measurements. The results of the simulations indicated that outward radial diffusion may significantly contribute to the variability of the radiation belt fluxes. However, both of these case studies used geosynchronous measurements at a fixed location in space which are highly affected by adiabatic changes. Measurements at a fixed L may produce up to 2 orders of magnitude underestimation of the L*-derived fluxes [e.g., *Desorgher et al.*, 2000]. Both of the studies did not specify a loss mechanism at higher L shells and did not consider the possibility of rapid losses to the atmosphere, e.g., caused by EMIC waves.

[8] *Green et al.* [2004] concluded that intense losses during the main phase of a storm cannot be produced by magnetopause encounters alone, since losses extended much further into the heart of the radiation belts than the estimated stormtime magnetopause location. In this study we attempt to verify whether negative gradients ($\partial f/\partial L^* < 0$) in phase space density, created by losses to the magnetopause, and consequent outward radial diffusion, are capable of contributing to the main phase depletions of the radiation belts, and thus produce the observed flux dropouts at lower L values.

[9] In section 2 we present SAMPEX observations of a 70 day period in October, November, and December 2003. We show that the flux dropouts are not adiabatic, and usually occur when the plasmapause is compressed and geomagnetic activity is high. To determine if the main phase dropouts are a result of scattering by EMIC waves or outward radial diffusion, we present multi energy Highly Elliptical Orbit (HEO) observations in section 3. To verify the feasibility and efficiency of the outward radial diffusion loss, we present radial diffusion simulations with a variable outer boundary (sections 4–6) and show how electron flux variations near geosynchronous orbit affect fluxes at lower L shells by means of outward or inward radial diffusion.

2. SAMPEX Observations

[10] Figure 1 shows the evolution of 2–6 MeV electron fluxes observed over 70 days by the Proton/Electron Telescope instrument on SAMPEX starting on day of year (DOY) 290, 2003 (17 October). The variability of the electron fluxes and the formation of a new radiation belt during these strong geomagnetic storms has been previously reported and studied by [*Baker et al.*, 2004; *Horne et al.*, 2005b; *Thorne et al.*, 2005a; *Shprits et al.*, 2006]. In this study we concentrate on stormtime depletions of the radiation belts during this time period. Part of the dropout in fluxes may be associated with adiabatic changes. For most of the storms shown on Figure 1, *Dst* recovers before the fluxes return to prestorm values which indicates that non-adiabatic losses occur during the main phases of the storms.

[11] If inward radial diffusion was the only acceleration mechanism, and it operated throughout the outer radiation zone, increases in ULF wave activity and corresponding increases in *Kp* should correspond to flux increases. In contrast, Figure 1 shows that each of the depletions (24, 29, and 31 October; 4 and 20 November; and 4 and 20 December, which correspond to DOY 297, 302, 304, 308, 324, 338, and 354), occurred when the *Kp* index suddenly increased. Such catastrophic decreases in fluxes during disturbed geomagnetic conditions could be explained either by increased EMIC wave activity and pitch angle scattering into a loss cone [*Summers and Thorne*, 2003; *Albert*, 2003], or could be due to the outward radial diffusion driven by losses to the magnetopause. As shown in Figure 1 (fourth panel), the solar wind dynamic pressure (*Dp*) increases for each of these events, causing a compression of magnetopause, and possible loss on the dayside. Figure 1 (fifth panel) shows the magnetopause standoff distance, estimated using the *Shue et al.* [1997] model, which moves inward in response to the increases in the solar wind dynamic pressure. Some of the magnetopause compressions, such as on 24 October (DOY 297) and 4 December (DOY 338), are not associated with a significant drop in *Dst* but clearly produce depletions in the outer radiation belt zone which again indicates that losses associated with increases in *Kp* and solar wind dynamic pressure are irreversible.

3. HEO Multichannel Observations

[12] Since EMIC waves only interact with electrons at energies $\geq$0.5 MeV [*Meredith et al.*, 2003; *Summers and Thorne*, 2003], precipitation loss from EMIC scattering can be separated from losses due to the outward radial diffusion by comparing the evolution of fluxes at various energies. Figure 2 shows Highly Elliptical Orbit (HEO) satellite

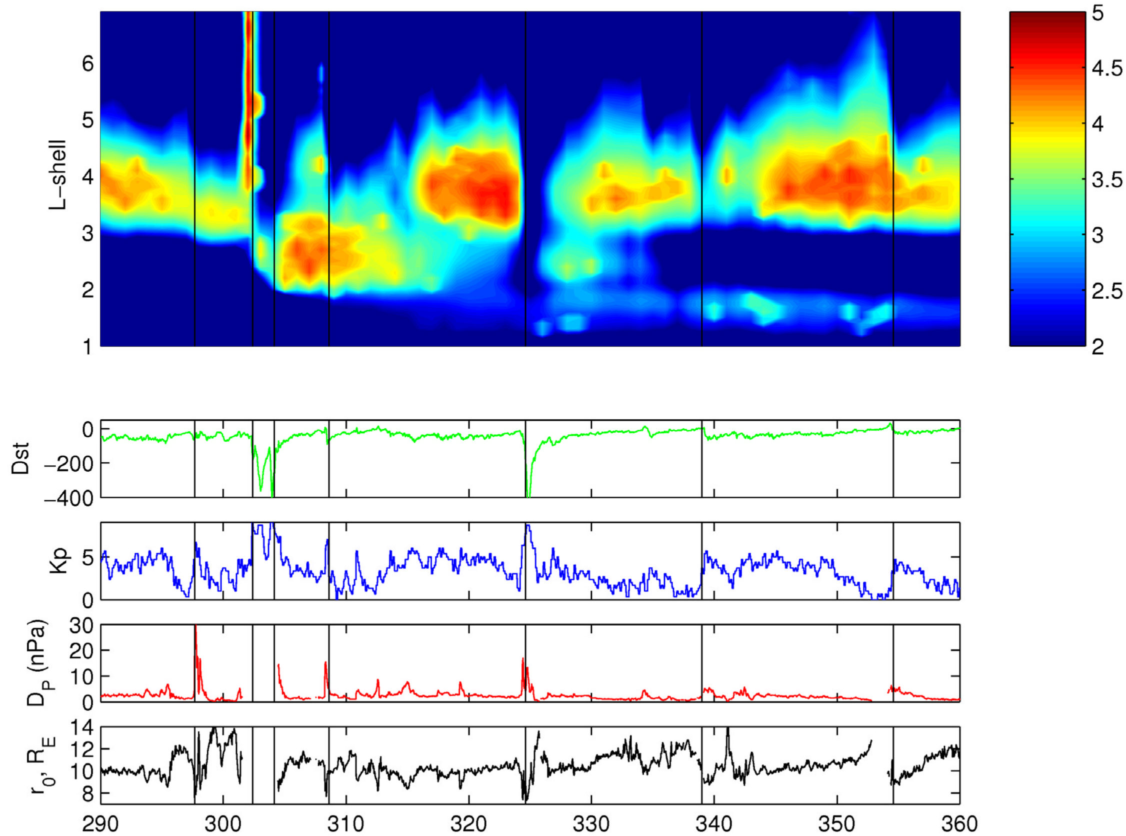

Figure 1. (first panel) SAMPEX observations of 2–6 MeV electron fluxes in $\log_{10}(\mathrm{cm}^{-2}\ \mathrm{sr}^{-1}\ \mathrm{s}^{-1})$ from 17 October until 26 December 2003. (second panel) Evolution of the *Dst* index, (third panel) *Kp*, (fourth panel) solar wind dynamic pressure inferred from ACE measurements in $\mathrm{km}^2\ \mathrm{s}^{-1}\ \mathrm{cm}^{-1}$, and (fifth panel) estimated magnetopause location.

observations in six energy channels ranging from $E >$ 0.13 MeV to $E >$ 3 MeV. The depletions of relativistic electrons are seen simultaneously on the low orbiting SAMPEX and the polar orbiting HEO spacecraft. The comparison of SAMPEX and HEO observations suggest that electron flux dropouts occur over a broad range of pitch angles and at all local times. For the same events as described in section 2, HEO observations show that all channels, (including $E >$ 0.13 and $E >$ 0.23 MeV) are depleted down to L = 4 during the main phases of the strong storms. For most of the storms, *Dst* recovers before the full recovery of fluxes, indicating that nonadiabatic loss occurs down to energies of hundreds of keV. Such loss cannot be explained by the EMIC wave scattering alone. However, EMIC waves may contribute to depletions at lower L values.

4. Variable Outer Boundary Conditions

[13] In this section we describe the variable outer boundary condition used for the simulations. Geosynchronous fluxes are highly affected by adiabatic changes, producing variations by as much as 3 orders of magnitude. These adiabatic changes can be filtered out by evaluating the phase space density as a function of the third adiabatic invariant or, equivalently, the L* parameter [*Roederer*, 1970]. Once phase space density is prescribed as a function of L*, all remaining flux variations must be caused by nonadiabatic loss or source processes. In the current study we evaluate fluxes at L* = 6 to prescribe an outer boundary condition for a radial diffusion model which accounts for the nonadiabatic changes.

[14] Figure 3 (top) shows the Combined Release and Radiation Effects Satellite (CRRES) measurements of 1.0 MeV electron fluxes at L* = 6, computed with T89 dynamic and OP77 static magnetic field models. Since data at L* = 7 are sparse, following *Brautigam and Albert* [2000], we use the normalized variation at L* = 6 and apply it to the average fluxes at L* = 7 to produce the variable boundary condition. Radial diffusion coefficients are very high near geosynchronous orbit, which tends to flatten phase space density [*Shprits and Thorne*, 2004]. Consequently, we can expect similar relative variation in fluxes for high L* values. Figure 3 (bottom) shows the evolution of the *Kp* index. Most of the strongest electron flux depletions at L* = 6 are associated with a sudden increase in *Kp*. CRRES measurements are confined to a narrow band of nearly equatorial pitch angles and will be used as a boundary condition for the radial diffusion model which treats only 90° pitch angle particles.

5. Model Description

[15] Conservation of the first and second adiabatic invariants results in acceleration of particles during the inward

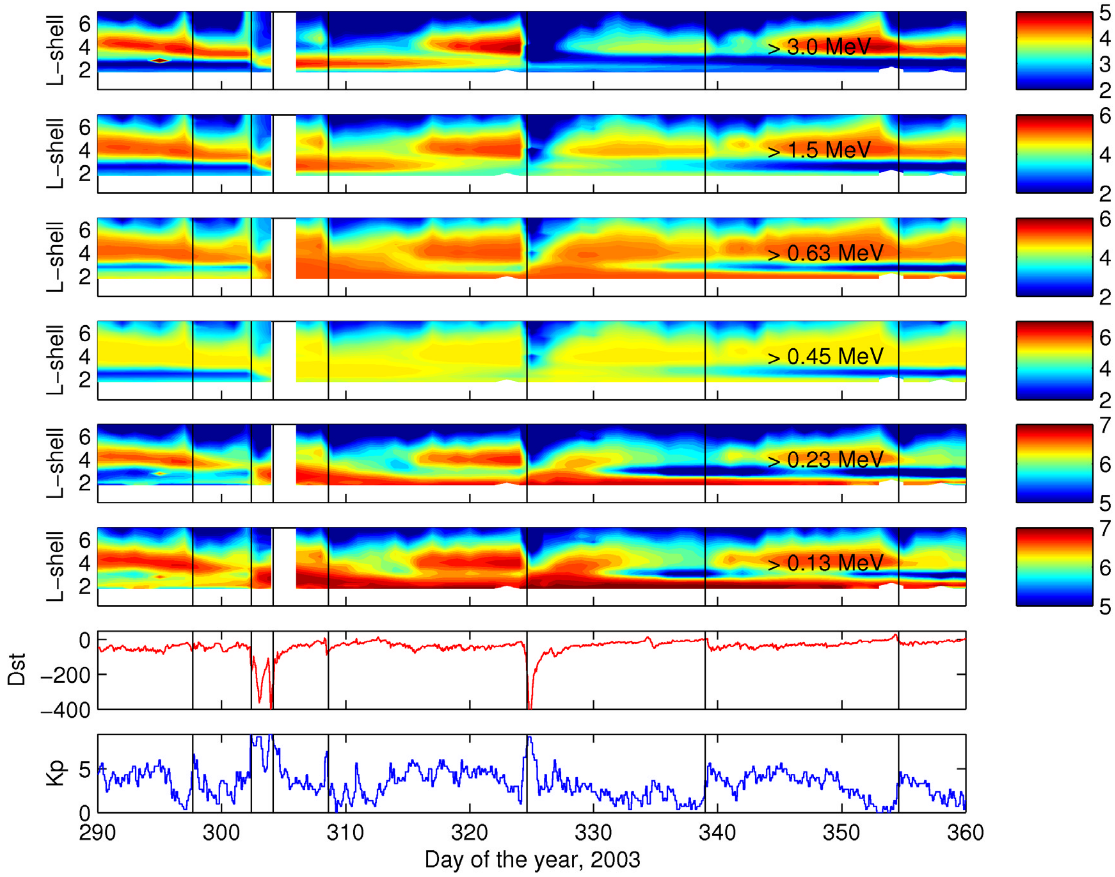

Figure 2. (first to sixth panels) Integrated electron flux measured on HEO for energies >3.0, 1.5, 0.63, 0.45, 0.23, and 0.13 MeV in $\log_{10}(\mathrm{cm}^{-2}\ \mathrm{sr}^{-1}\ \mathrm{s}^{-1})$ and (seventh and eighth panels) *Dst* and the *Kp* index.

transport and deceleration during the outward transport. The direction of the net diffusive flux is opposite to the radial gradient in phase space density. The net diffusive flux depends on the diffusion coefficients and the gradient in phase space density. If local acceleration is ignored, the temporal evolution of phase space density can be obtained from [*Schulz and Lanzerotti*, 1974]

$$\frac{\partial f}{\partial t} = L^2 \frac{\partial}{\partial L}\left[D_{LL} L^{-2} \frac{\partial f}{\partial L}\right] - \frac{f}{\tau}, \quad (1)$$

where τ is the electron lifetime and D_{LL} is the radial diffusion coefficient. In this formulation the first two adiabatic invariants μ and J are held constant, and equation (1) can be solved numerically for $f(L, t)$. In the present study we adopt an empirical relationship for the rate of radial diffusion due to magnetic fluctuations [*Brautigam and Albert*, 2000], which tends to dominate throughout the outer radiation zone

$$D_{LL}^{M}(Kp, L) = 10^{(0.506Kp - 9.325)} L^{10} \mathrm{d}^{-1}, \; Kp = 1 \text{ to } 6. \quad (2)$$

Solutions of the time-dependent code, ignoring the effects of local acceleration and only considering radial diffusion with losses, are compared to CRRES Medium Electrons A (MEA) electron spectrometer observations.

[16] The inner boundary for our simulation $f(L = 1) = 0$ is taken to represent loss to the atmosphere. Following [*Shprits and Thorne*, 2004], we model fluxes by an exponential fit $J = 8222.6 {*} \exp(-7.068K)\ \mathrm{cm}^{-2}\ \mathrm{sr}^{-1}\ \mathrm{keV}^{-1}\ \mathrm{s}^{-1}$, where K is kinetic energy in (MeV). Variable outer boundary conditions were described in section 4. For simplicity, we first assume that the diffusion coefficients and lifetimes are independent of energy and solve equation (1) for $f(L, t)$, normalized to unity at the outer boundary. This solution will be the same for all μ values. Consequently, to obtained $f(E, L)$, the normalized phase space density should be multiplied by $J(E^*)/p^{*2}$, where E^* and p^* are the kinetic energy and momentum of the particles adiabatically scaled to the outer boundary and J is a differential flux at the outer boundary. *Shprits et al.* [2005] showed that for simulations with constant outer boundary conditions, parameterizations of lifetime $\tau = 3/Kp$ is optimum for reproducing observations. Since maximum radial diffusion rates during storms occur when the outer zone fluxes are most depleted, introduction of the variable boundary results in a lower net diffusive flux. For simulations with variable outer boundary, lifetime parameterizations $\tau = 5/Kp$ produced best agreement with CRRES observations in terms of the location of the peak of fluxes and the radial extent of fluxes. Furthermore, since chorus scattering rates do not show significant

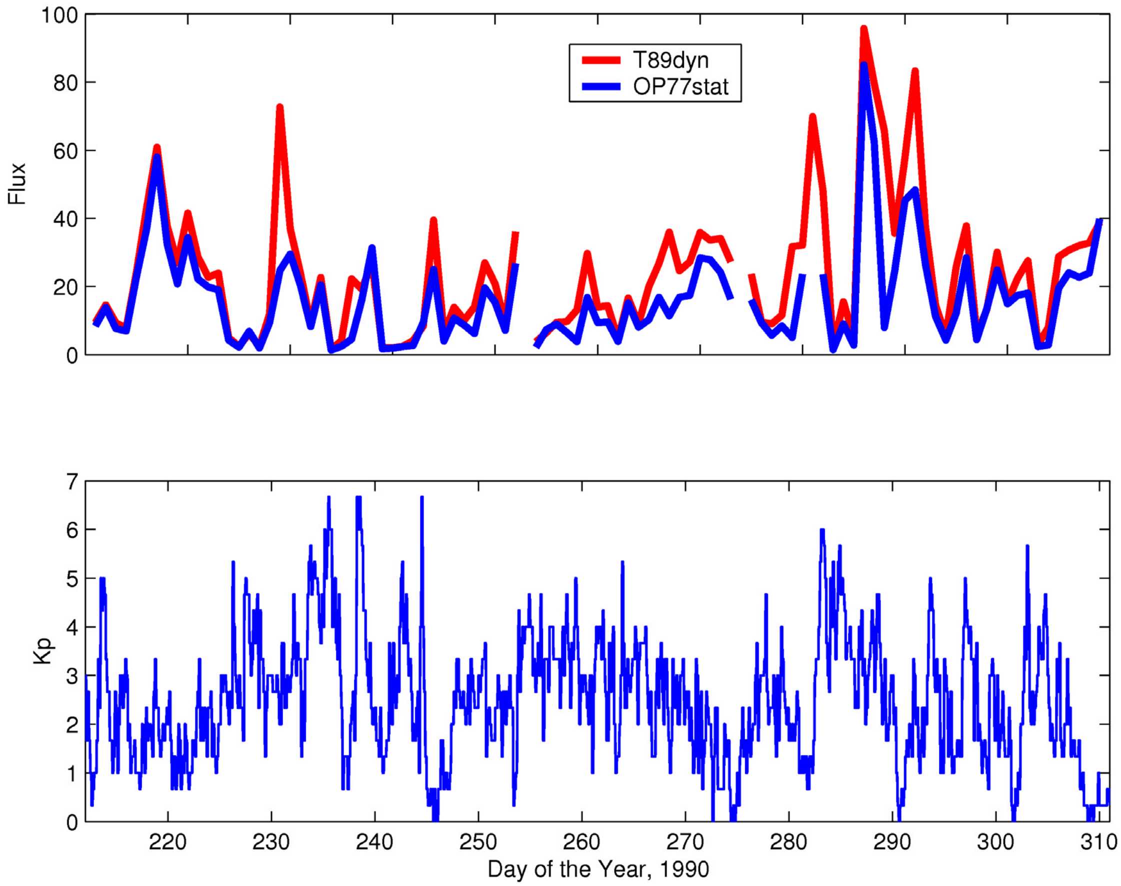

Figure 3. (top) Daily averages of the 1 MeV electron fluxes at $L^* = 6$, measured on CRRES (cm^{-2} sr^{-1} s^{-1} keV). The L^* parameter was derived using the T89 dynamic and OP77 static models. (bottom) Evolution of the *Kp* index.

L dependence [*Thorne et al.*, 2005b], we adopt a lifetime parameter independent of *L*.

6. Simulations With Variable and Constant Outer Boundary

[17] To verify that outward radial diffusion, driven by outer boundary variations around geosynchronous orbit (for example, due to the losses at magnetopause), can produce significant depletions in the heart of the radiation belts, we conducted numerical simulations with both variable and constant outer boundary conditions as described in section 4. We choose a modeling period from 19 July 1990 (DOY 210) until 6 November 1990 (DOY 310) and compare results of the radial diffusion simulation to CRRES measurements at 1 MeV. During this time *Kp* was less than 6 for which diffusion coefficients (2) are valid. Figure 4 (first panel) shows radial diffusion simulations with constant outer boundary conditions. Our radial diffusion model predicts almost instantaneous increases in the 1 MeV fluxes during the main phase of the storm when diffusion coefficients maximize. In contrast, CRRES observations (Figure 4, second panel) show depletions during the main phase of the storms. Results of the simulations with variable outer boundary (Figure 4, fourth panel) are in a better agreement with observations at high *L* shells. Enhanced radial diffusion down to $L = 4$ causes fluxes to respond rapidly to outer boundary variations. We conclude that nonadiabatic flux variations near the boundary of trapping (possibly due to magnetopause losses) together with outward radial diffusion are capable of explaining the main phase depletions in the radiation belts down to $L = 4$. The differences between model results and observations may be due to the neglect of EMIC wave scattering which could provide additional losses at lower *L*, and the neglect of the chorus wave scattering which may locally accelerate electrons in the region outside the plasmapause [*Horne et al.*, 2005a].

7. Summary and Discussion

[18] The HEO, SAMPEX, and CRRES observations presented above indicate that main phase depletions occur when the magnetopause is compressed and *Kp* index (used as a proxy of the ULF activity) is high. EMIC wave scattering alone cannot explain radiation belt depletions at higher *L* shells, which occur down to a few hundred keV, below the EMIC minimum resonant energies. However, EMIC scattering may contribute to loss at lower *L* shells. Comparison between the radial diffusion simulations and CRRES MEA observations indicate that radial diffusion is fast and efficient enough to propagate outer boundary variations down to $L = 4–5$ and thus may explain nonadiabatic dropouts during the storm-time conditions. Outward radial diffusion may also be an important loss and source

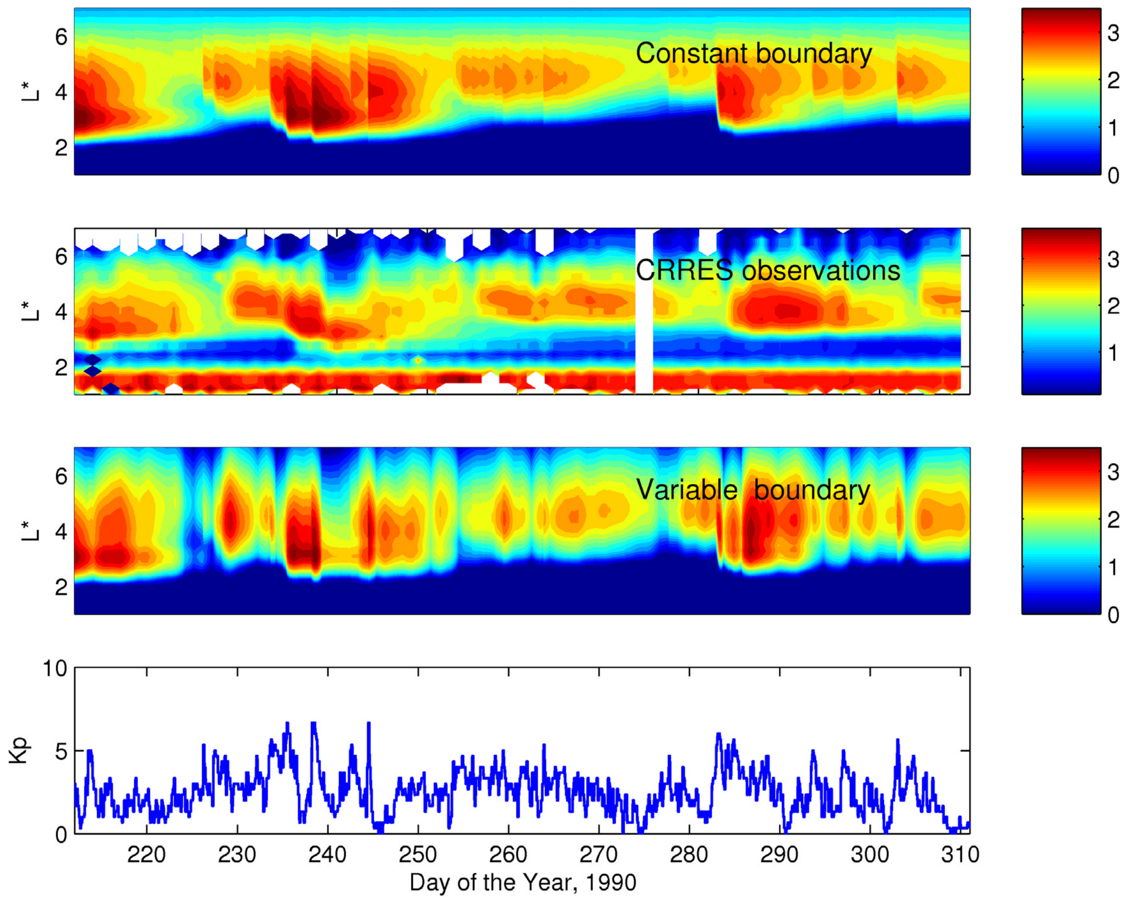

Figure 4. (first panel) The 1.0 MeV electron fluxes computed with the radial diffusion code and constant outer boundary. (second panel) CRRES MEA observations of 1 MeV electron fluxes. (third panel) Radial diffusion simulations with variable outer boundary. Differential flux is color-coded in $\log_{10}(\mathrm{cm}^{-2}\ \mathrm{sr}^{-1}\ \mathrm{s}^{-1}\ \mathrm{keV}^{-1})$. (fourth panel) Evolution of the *Kp* index. Time interval from 19 July 1990 (DOY 210) until 6 November 1990 (DOY 310).

process when the peak in the radiation belts is formed by local acceleration [*Green and Kivelson*, 2004]. In this case, radial diffusion works as a loss outside of the peak in phase space density and will accelerate electrons inside of the peak [*Varotsou et al.*, 2005].

[19] The results of our simulations indicate that radial diffusion can effectively redistribute outer radiation belt fluxes and smooth PSD gradients, which are produced by losses to magnetopause and convection of plasma sheet electrons or by local acceleration and loss. Our results clearly show that radial diffusion is very effective in transporting relativistic electrons across the *L* shells but raise serious questions on the effectiveness of inward radial diffusion from the plasma sheet as the major source of relativistic electrons. During some storms local acceleration driven by chorus emissions can be more effective [*Horne et al.*, 2005b; *Shprits et al.*, 2006] and can produce local peaks in phase space density just outside the plasmapause. Electrons are subsequently transported inward or outward by radial diffusion. Future research should be directed at quantifying the relative role of either diffusive radial transport or local acceleration in causing stormtime variability in the radiation belts.

[20] **Acknowledgments.** Work at UCLA was supported in part by IGPP LANL Collaborative Research minigrant, NASA grants NNX06AB84G and NNG04GN44G, and NSF GEM grant ATM-0603191. Work at the Aerospace Corporation was supported by the LWS DATM grant NAG5-10972. Work at Los Alamos was supported by NASA LWS program and the U.S. Department of Energy DREAM project.

[21] Amitava Bhattacharjee thanks Alexander Vapirev and another reviewer for their assistance in evaluating this paper.

References

Abel, B., and R. M. Thorne (1998), Electron scattering loss in Earth's inner magnetosphere: 1. Dominant physical processes, *J. Geophys. Res.*, *103*, 2385–2396.

Albert, J. M. (1994), Quasi-linear pitch angle diffusion coefficients: Retaining high harmonics, *J. Geophys. Res.*, *99*, 23,741–23,746.

Albert, J. M. (2003), Evaluation of quasi-linear diffusion coefficients for EMIC waves in a multispecies plasma, *J. Geophys. Res.*, *108*(A6), 1249, doi:10.1029/2002JA009792.

Albert, J. M. (2005), Evaluation of quasi-linear diffusion coefficients for whistler mode waves in a plasma with arbitrary density ratio, *J. Geophys. Res.*, *110*, A03218, doi:10.1029/2004JA010844.

Baker, D. N., S. G. Kanekal, X. Li, S. P. Monk, J. Goldstein, and J. L. Burch (2004), An extreme distortion of the Van Allen belt arising from the Halloween solar storm in 2003, *Nature*, 878–880.

Brautigam, D. H., and J. M. Albert (2000), Radial diffusion analysis of outer radiation belt electrons during the October 9, 1990, magnetic storm, *J. Geophys. Res.*, *105*, 291–310.

Desorgher, L., P. Bühler, A. Zehnder, and E. O. Flückiger (2000), Simulation of the outer radiation belt electron flux decrease during the March 26, 1995, magnetic storm, *J. Geophys. Res.*, *105*, 21,211–21,224.

Erlandson, R. E., and A. J. Ukhorskiy (2001), Observations of electromagnetic ion cyclotron waves during geomagnetic storms: Wave occurrence and pitch angle scattering, *J. Geophys. Res.*, *106*, 3883–3896.

Green, J. C., and M. G. Kivelson (2004), Relativistic electrons in the outer radiation belt: Differentiating between acceleration mechanisms, *J. Geophys. Res.*, *109*, A03213, doi:10.1029/2003JA010153.

Green, J. C., T. G. Onsager, T. P. O'Brien, and D. N. Baker (2004), Testing loss mechanisms capable of rapidly depleting relativistic electron flux in the Earth's outer radiation belt, *J. Geophys. Res.*, *109*, A12211, doi:10.1029/2004JA010579.

Horne, R. B., and R. M. Thorne (1993), On the preferred source location for the convective amplification of ion cyclotron waves, *J. Geophys. Res.*, *98*, 9233–9248.

Horne, R. B., and R. M. Thorne (1997), Wave heating of He^+ by electromagnetic ion cyclotron waves in the magnetosphere: Heating near the H^+–He^+ bi-ion resonance frequency, *J. Geophys. Res.*, *102*, 11,457–11,472.

Horne, R. B., R. M. Thorne, S. A. Glauert, J. M. Albert, N. P. Meredith, and R. R. Anderson (2005a), Timescale for radiation belt electron acceleration by whistler mode chorus waves, *J. Geophys. Res.*, *110*, A03225, doi:10.1029/2004JA010811.

Horne, R. B., et al. (2005b), A critical test of electron acceleration in the Van Allen radiation belts, *Nature*, *437*, 227–230, doi:10.1038/nature03939.

Jordanova, V. K., C. J. Farrugia, R. M. Thorne, G. V. Khazanov, G. D. Reeves, and M. F. Thomsen (2001a), Modeling ring current proton precipitation by electromagnetic ion cyclotron waves during the May 14–16, 1997, storm, *J. Geophys. Res.*, *106*, 7–22.

Jordanova, V. K., R. M. Thorne, C. J. Farrugia, Y. Dotan, J. F. Fennell, M. F. Thomsen, G. D. Reeves, and D. J. McComas (2001b), Ring current dynamics during the July 13–18, 2000 storm period, *Sol. Phys.*, *204*, 361–375.

Kim, H. J., and A. A. Chan (1997), Fully adiabatic changes in stormtime relativistic electron fluxes, *J. Geophys. Res.*, *102*, 22,107–22,116.

Kozyra, J. U., et al. (1997), Modeling of the contribution of electromagnetic ion cyclotron (EMIC) waves to stormtime ring current erosion, in *Magnetic Storms*, *Geophys. Monogr. Ser.*, vol. 98, edited by B. T. Tsurutani et al., p. 187, AGU, Washington, D. C.

Li, X., D. N. Baker, M. Temerin, T. E. Cayton, E. G. D. Reeves, R. A. Christensen, J. B. Blake, M. D. Looper, R. Nakamura, and S. G. Kanekal (1997), Multisatellite observations of the outer zone electron variation during the November 3–4, 1993, magnetic storm, *J. Geophys. Res.*, *102*, 14,123–14,140.

Lorentzen, K. R., M. P. McCarthy, G. K. Parks, J. E. Foat, R. M. Millan, D. M. Smith, R. P. Lin, and J. P. Treilhou (2000), Precipitation of relativistic electrons by interaction with electromagnetic ion cyclotron waves, *J. Geophys. Res.*, *105*, 5381–5390.

Lorentzen, K. R., J. B. Blake, U. S. Inan, and J. Bortnik (2001), Observations of relativistic electron microbursts in association with VLF chorus, *J. Geophys. Res.*, *106*, 6017–6028.

Lyons, L. R., R. M. Thorne, and C. F. Kennel (1972), Pitch angle diffusion of radiation electrons within the plasmasphere, *J. Geophys. Res.*, *77*, 3455–3474.

Mathie, R. A., and I. R. Mann (2000), A correlation between extended intervals of ULF wave power and storm-time geosynchronous relativistic electron flux enhancements, *Geophys. Res. Lett.*, *27*, 3261–3264.

McAdams, K. L., and G. D. Reeves (2001), Non-adiabatic response of relativistic radiation belt electrons to GEM magnetic storms, *Geophys. Res. Lett.*, *28*, 1879–1882.

Meredith, N. P., R. M. Thorne, R. B. Horne, D. Summers, B. J. Fraser, and R. R. Anderson (2003), Statistical analysis of relativistic electron energies for cyclotron resonance with EMIC waves observed on CRRES, *J. Geophys. Res.*, *108*(A6), 1250, doi:10.1029/2002JA009700.

Meredith, N. P., R. B. Horne, R. M. Thorne, D. Summers, and R. R. Anderson (2004), Substorm dependence of plasmaspheric hiss, *J. Geophys. Res.*, *109*, A06209, doi:10.1029/2004JA010387.

Millan, R. M., R. P. Lin, D. M. Smith, K. R. Lorentzen, and M. P. McCarthy (2002), X-ray observations of MeV electron precipitation with a balloon-borne germanium spectrometer, *Geophys. Res. Lett.*, *29*(24), 2194, doi:10.1029/2002GL015922.

Miyoshi, Y., A. Morioka, T. Obara, H. Misawa, T. Nagai, and Y. Kasahara (2003), Rebuilding process of the outer radiation belt during the 3 November 1993 magnetic storm: NOAA and Exos-D observations, *J. Geophys. Res.*, *108*(A1), 1004, doi:10.1029/2001JA007542.

Nagai, T. (1988), ''Space weather forecast'': Prediction of relativistic electron intensity at synchronous orbit, *Geophys. Res. Lett.*, *15*, 425–428.

O'Brien, T. P., R. L. McPherron, D. Sornette, G. D. Reeves, R. Friedel, and H. J. Singer (2001), Which magnetic storms produce relativistic electrons at geosynchronous orbit?, *J. Geophys. Res.*, *106*, 15,533–15,544.

O'Brien, T. P., M. D. Looper, and J. B. Blake (2004), Quantification of relativistic electron microbursts losses during the GEM storms, *Geophys. Res. Lett.*, *31*, L04802, doi:10.1029/2003GL018621.

Onsager, T. G., G. Rostoker, H.-J. Kim, G. D. Reeves, T. Obara, H. J. Singer, and C. Smithtro (2002), Radiation belt electron flux dropouts: Local time, radial, and particle-energy dependence, *J. Geophys. Res.*, *107*(A11), 1382, doi:10.1029/2001JA000187.

Reeves, G. D., et al. (1998), The global response of relativistic radiation belt electrons to the January 1997 magnetic cloud, *Geophys. Res. Lett.*, *25*, 3265–3268.

Reeves, G. D., K. L. McAdams, R. H. W. Friedel, and T. P. O'Brien (2003), Acceleration and loss of relativistic electrons during geomagnetic storms, *Geophys. Res. Lett.*, *30*(10), 1529, doi:10.1029/2002GL016513.

Roederer, J. G. (1970), *Dynamics of Geomagnetically Trapped Radiation*, Springer, New York.

Schulz, M., and L. J. Lanzerotti (1974), *Physics and Chemistry in Space*, vol. 7, *Particle Diffusion in the Radiation Belts*, Springer, New York.

Shprits, Y. Y., and R. M. Thorne (2004), Time dependent radial diffusion modeling of relativistic electrons with realistic loss rates, *Geophys. Res. Lett.*, *31*, L08805, doi:10.1029/2004GL019591.

Shprits, Y. Y., R. M. Thorne, G. D. Reeves, and R. Friedel (2005), Radial diffusion modeling with empirical lifetimes: Comparison with CRRES observations, *Ann. Geophys.*, *23*, 1467–1471.

Shprits, Y. Y., R. M. Thorne, R. B. Horne, S. A. Glauert, M. Cartwright, C. T. Russell, D. N. Baker, and S. G. Kanekal (2006), Acceleration mechanism responsible for the formation of the new radiation belt during the 2003 Halloween solar storm, *Geophys. Res. Lett.*, *33*, L05104, doi:10.1029/2005GL024256.

Shue, J.-H., J. K. Chao, H. C. Fu, C. T. Russell, P. Song, K. K. Khurana, and H. J. Singer (1997), A new functional form to study the solar wind control of the magnetopause size and shape, *J. Geophys. Res.*, *102*, 9497–9512.

Summers, D., and R. M. Thorne (2003), Relativistic electron pitch-angle scattering by electromagnetic ion cyclotron waves during geomagnetic storms, *J. Geophys. Res.*, *108*(A4), 1143, doi:10.1029/2002JA009489.

Thorne, R. M., and C. F. Kennel (1971), Relativistic electron precipitation during magnetic storm main phase, *J. Geophys. Res.*, *76*, 4446–4453.

Thorne, R. M., R. B. Horne, S. Glauert, N. P. Meredith, Y. Y. Shprits, D. Summers, and R. Anderson (2005a), The influence of wave-particle interactions on relativistic electron dynamics during storms, in *Inner Magnetosphere Interaction: New Perspectives From Imaging*, *Geophys. Monogr. Ser.*, vol. 159, edited by J. Burch, M. Schulz, and H. Spence, pp. 101–112, AGU, Washington D. C.

Thorne, R. M., T. P. O'Brien, Y. Y. Shprits, D. Summers, and R. B. Horne (2005b), Timescale for MeV electron microburst loss during storms, *J. Geophys. Res.*, *110*, A09202, doi:10.1029/2004JA010882.

Varotsou, A., D. Boscher, S. Bourdarie, R. B. Horne, S. A. Glauert, and N. P. Meredith (2005), Simulation of the outer radiation belt electrons near geosynchronous orbit including both radial diffusion and resonant interaction with Whistler-mode chorus waves, *Geophys. Res. Lett.*, *32*, L19106, doi:10.1029/2005GL023282.

D. N. Baker and S. G. Kanekal, Laboratory for Atmospheric and Space Physics, University of Colorado, 1234 Innovation Drive, Boulder, CO 80303-7814, USA.

J. Fennell, The Aerospace Corp., Mail Stop M2-259, P.O. Box 92957, Los Angeles, CA 90009, USA.

R. Friedel and G. D. Reeves, Los Alamos National Laboratory, Mail Stop D436, Los Alamos, NM 87545, USA.

Y. Y. Shprits and R. M. Thorne, Department of Atmospheric and Oceanic Sciences, University of California, 405 Hilgard Ave., Box 951565, 7127 Math Sciences Bldg., Los Angeles, CA 90095-1565, USA. (yshprits@atmos.ucla.edu)